

A Method for Simplifying the Analysis of Leg-Based Visual Servoing of Parallel Robots

Victor Rosenzweig^{1,2}, Sébastien Briot¹, Philippe Martinet^{1,2}, Erol Özgür³, and Nicolas Bouton³

Abstract—As the end-effector pose is an external property of a parallel robot, it is natural to use exteroceptive sensors to measure it in order to suppress inaccuracies coming from modelling errors. Cameras offer this possibility. So, it is possible to obtain higher accuracy than in the case of classic control schemes (based on geometrical model).

In some cases, it is impossible to directly observe the end-effector, but the leg directions can instead be used. In this case, however, unusual results were recorded, namely: (i) the possibility of controlling the robot by observing a number of legs less than the total number of legs, and that (ii) in some cases, the robot does not converge to the desired end-effector pose, even if the observed leg directions did.

These results can be explained through the use of the hidden robot concept, which is a tangible visualisation of the mapping between the observed leg direction space (internal property) and Cartesian space (external property). This hidden robot has different assembly modes and singular configurations from the real robot, and it is a powerful tool to simplify the analysis of the aforementioned mapping.

In this paper, the concept of hidden robot model is generalised for any type of parallel robot controlled through visual servoing based on observation of the leg directions.

Validation has been accomplished through experiments on a Quattro robot with 4 dof.

I. INTRODUCTION

Compared to serial robots, parallel kinematic manipulators [1] are stiffer and can reach higher speeds and accelerations [2]. However, their control is troublesome because of the complex mechanical structure, highly coupled joint motions and many other factors (e.g. clearances, assembly errors, etc.) which degrade stability and accuracy.

Many research papers focus on the control of parallel mechanisms (see [3] for a long list of references). It may be possible to bypass the complex kinematic structure of the robot and to apply a form of control which uses an external sensor to estimate the pose of the end-effector, reducing the stability and accuracy degradation mentioned earlier.

This work was supported by the French ANR project ARROW (ANR-2011BS3-006-01), by the French ANR project EquipEx RobotEx (ANR-10-EQPX-44) and by the European Union Program “Compétitivité Régionale et Emploi 2007–2013” (FEDER – Région Auvergne).

The authors would like to thank Michel Coste from the Institut de Recherche Mathématique de Rennes (University of Rennes, France) for his smart advices about the use of the Bézout theorem and the definition of the Bohemian Dome.

¹V. Rosenzweig, S. Briot, and P. Martinet are with Institut de Recherches en Communications et Cybernétique de Nantes (IRCCyN), UMR CNRS 6597, Nantes, France

²V. Rosenzweig and P. Martinet are with LUNAM University, École Centrale de Nantes, Nantes, France

³E. Özgür and N. Bouton are with Institut Français de Mécanique Avancée (IFMA), Institut Pascal, UMR CNRS 6602, Clermont-Ferrand, France

A proven approach for estimating the end-effector pose is through the use of vision. The most common approach consists of the direct observation of the end-effector pose [4], [5], [6]. In some cases, however, it may prove difficult or unwise to observe the end-effector of the robot, e.g. in the case of a machine-tool. A substitute target for the observation must then be chosen and an effective candidate for this are the legs of the robot, which are usually designed with slim and rectilinear rods [3]. When moving the object of observation from the end-effector to the robot legs, the result of the observation becomes a direct measure of an internal property, i.e. the kinematic configuration of the robot. In addition, as the information is acquired through an external sensor, this technique allows to estimate indirectly the pose of the end-effector from it (like it is done in [7]) which is an external property.

An application of this technique was performed in [8] where vision was used to derive a visual servoing scheme based on the observation of a Gough-Stewart (GS) parallel robot [9]. In that method, the leg directions were chosen as visual primitives and control was derived based on their reconstruction from the image. The approach was applied to several types of robots, such as the Adept Quattro and other robots of the same family [10], [11].

However, two unexpected results arose from the application of this technique:

- It was possible to control the robot by observing a number of legs fewer than the total number of legs. This is surprising because in the case of standard control schemes (actuator-based control), each actuated leg has to be controlled in order to fully servo the robot (six legs for the GS platform using actuators, instead of three legs using vision; four legs for the Quattro using actuators, instead of two legs using vision).
- In some cases, the robot did not converge to the desired pose, even if all observed leg directions did. This was surprising, since the whole idea of using an external sensor is to get the exact position of the end-effector.

Not only were these two points inexplicable, but other questions arose too, which were never answered. Such as:

- Are we sure there are no local minima (for which the error in the observation space is non zero while the robot platform cannot move [12]) in the Cartesian space?
- Are we sure that there is no singularity in the mapping between the leg direction space and the Cartesian space?

Due to the unusual nature of this visual servoing technique, all these points were left unanswered. It was clear that this

behaviour was due to the mapping between Cartesian space and the leg direction observation space, but at this time the nature of the mapping was not understood and *there were no tools available* to analyse correlation between the intrinsic and extrinsic properties of the controller.

The answer came only recently, when two of the authors of the present paper proposed the existence of a virtual robot model “hidden” within the controller. This robot presents singular configurations and assembly modes different from the controlled robot, and it is this hidden robot whose intrinsic and extrinsic properties are being used through the observation of the real robot’s leg directions.

This proposition was demonstrated in [13] where the visual servoing of the leg directions of the GS platform was proven to be equivalent to controlling the hidden 3-UPS¹ robot. A similar property has been shown for the control of the Adept Quattro *with only 3 translational degrees of freedom (dof* – a redundant version of the Quattro with a rigid platform) for which another hidden robot model, completely different from the one of the GS platform, has been found [15].

In both cases, the hidden virtual robot is proven to be a tangible visualisation of the mapping between the observation space and the real robot Cartesian space, correlating the external and internal properties observed through vision. Considering this hidden robot model, a minimal representation for the leg observation-based control of the studied robots can be found, which makes it possible to answer the previous questions.

Thus, the concept of hidden robot model, is *the* tool able to analyse the intrinsic properties of some controllers developed by the visual servoing community, without which the behaviour of the controller cannot fully be explained. Moreover, this concept shows that in some visual servoing approaches, using only the extrinsic properties and stacking several interaction matrices to derive a control scheme without doing a deep analysis of the intrinsic properties of the controller is clearly not enough. Further investigations are required.

Therefore, in this paper, the generalization of the concept of hidden robot model is presented and a general way to find the hidden robots corresponding to any kind of robot architecture is explained. It will be shown that the concept of hidden robot model is a powerful tool which correlates the extrinsic and intrinsic properties observed through the visual servoing of robots using leg direction observation and gives useful insights about this kind of visual servoing technique. Not only does the concept of hidden robot model answer the unexplained results presented earlier, but also through its use the singularity problem of the mapping between the space of the observed robot links and the Cartesian space can be addressed. Moreover, it is possible to give and certify information, in a simplified way, about the controllability of the observed robots using the proposed controller.

¹In the following of the paper, R , P , U , S , Π will stand for passive revolute, prismatic, universal, spherical and planar parallelogram joint [14], respectively. If the letter is underlined, the joint is considered active.

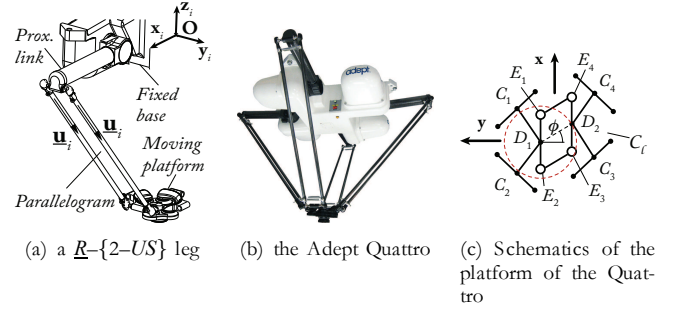


Fig. 1. Example of leg, robot, and platform for the Adept Quattro

II. RECALLS ON VISUAL SERVOING OF PARALLEL ROBOTS USING LEG OBSERVATIONS

The proposed control approach was to servo the leg directions ${}^c\mathbf{u}_i$ [8] (Fig. 1(a)). Some brief recalls on this type of controller are done below.

A. Interaction matrix

Visual servoing is based on the so-called interaction matrix \mathbf{L}^T [16] which relates the instantaneous relative motion $T_c = {}^c\tau_c - {}^c\tau_s$ between the camera and the scene, to the time derivative of the vector s of all the visual primitives that are used through:

$$\dot{s} = \mathbf{L}_{(s)}^T T_c \quad (1)$$

where ${}^c\tau_c$ and ${}^c\tau_s$ are respectively the kinematic screw of the camera and the scene, both expressed in \mathcal{R}_c , i.e. the camera frame.

In the case where we want to directly control the leg directions ${}^c\mathbf{u}_i$, and if the camera is fixed, (1) becomes:

$${}^c\dot{\mathbf{u}}_i = \mathbf{M}_i^T {}^c\tau_c \quad (2)$$

where \mathbf{M}_i^T is the interaction matrix for the leg i .

B. Control

For the visual servoing of a robot, one achieves exponential decay of an error $e(s, s_d)$ between the current primitive vector s and the desired one s_d using a proportional linearizing and decoupling control scheme of the form:

$$T_c = \lambda \hat{\mathbf{L}}_{(s)}^{T+} e(s, s_d) \quad (3)$$

where T_c is used as a pseudo-control variable and the superscript “+” corresponds to the matrix pseudo-inverse.

The visual primitives being unit vectors, it is theoretically more elegant to use the geodesic error rather than the standard vector difference. Consequently, the error grounding the proposed control law will be:

$$\mathbf{e}_i = {}^c\mathbf{u}_i \times {}^c\mathbf{u}_{di} \quad (4)$$

where ${}^c\mathbf{u}_{di}$ is the desired value of ${}^c\mathbf{u}_i$.

It can be proven that, for spatial parallel robots, matrices \mathbf{M}_i are in general of rank 2 [8] (for planar parallel robots, they are of rank 1). As a result, for spatial robots with more than 2 *dof*, the observation of several independent legs is necessary to control the end-effector pose. An interaction

matrix \mathbf{M}^T can then obtained by stacking k matrices \mathbf{M}_i^T of k legs.

Finally, a control is chosen such that \mathbf{e} , the vector stacking the errors \mathbf{e}_i associated to of k legs ($k = 3 \dots 6$), decreases exponentially, i.e. such that

$$\dot{\mathbf{e}} = -\lambda \mathbf{e} \quad (5)$$

Then, introducing $\mathbf{L}_i^T = -[{}^c\mathbf{u}_{di}]_{\times} \mathbf{M}_i^T$, where $[{}^c\mathbf{u}_{di}]_{\times}$ is the cross product matrix associated with the vector ${}^c\mathbf{u}_{di}$, the combination of (4), (2) and (5) gives

$${}^c\tau_c = -\lambda \mathbf{L}^T \mathbf{e} \quad (6)$$

where \mathbf{L}^T can be obtained by stacking the matrices \mathbf{L}_i^T of k legs. The conditions for the rank deficiency of matrix \mathbf{L}^T , as well as the conditions that lead to local minima [12] of the Eq. (6) are discussed in Section III.

This expression can be transformed into the control joint velocities:

$$\dot{\mathbf{q}} = -\lambda {}^c\mathbf{J}^{inv} \mathbf{L}^T \mathbf{e} \quad (7)$$

where ${}^c\mathbf{J}^{inv}$ is the inverse Jacobian matrix of the robot relating the end-effector twist to the actuator velocities, i.e. ${}^c\mathbf{J}^{inv} {}^c\tau_c = \dot{\mathbf{q}}$.

In the next Section, it is shown that such type of controller involve the use of hidden robot models that can be studied for analysing the controllability of parallel robots using the proposed visual servoing approach.

III. THE CONCEPT OF HIDDEN ROBOT MODEL

The concept of hidden robot model has been first introduced in [13] for the visual servoing of the GS platform. In this paper, it has been demonstrated that the leg direction based visual servoing of such robots intrinsically involves the appearance of a hidden robot model, which has assembly modes and singularities different from the real robot. It was shown that the concept of hidden robot model fully explains the possible nonconvergence of the observed robot to the desired final pose and that it considerably simplifies the singularity analysis of the mapping involved in the controller.

The concept of hidden robot model comes from the following observation: in the classical control approach, the encoders measure the motion of the actuator; in the previously described control approach (Section II), the leg directions or leg edges are observed. So, in a reciprocal manner, one could wonder to what kind of virtual actuators such observations correspond. The main objective of this Section is to give a general answer to this question.

A. How to define the legs of the hidden robots

Let us consider a general leg for a parallel robot in which the direction \mathbf{u}_i of a segment is observed (Fig. 2(a) – in this figure, the last segment is considered observed, but the following explanations can be generalized to any segment located in the leg chain).

In the general case, the unit vector \mathbf{u}_i can obviously be parameterized by two independent coordinates, that can be two angles, for example the angles α and β of Fig. 2(c) defined such that $\cos \alpha = \mathbf{x} \cdot \mathbf{v} = \mathbf{y} \cdot \mathbf{w}$ (where \mathbf{v} and \mathbf{w} are

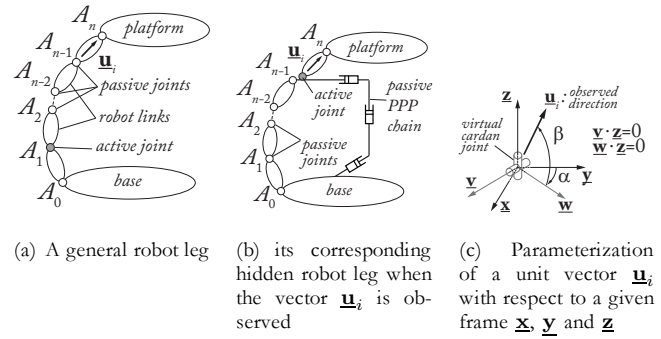


Fig. 2. A general robot leg and its corresponding hidden robot leg when the vector \mathbf{u}_i is observed, and parametrization of said vector

defined such that $\mathbf{z} \cdot \mathbf{v} = \mathbf{z} \cdot \mathbf{w} = 0$) and $\cos \beta = \mathbf{u}_i \cdot \mathbf{x}$. Thus α is the angle of the first rotation of the link direction \mathbf{u}_i around \mathbf{z} and β is the angle of the second rotation around \mathbf{v} .

It is well known that a U joint is able to orientate a link around two orthogonal axes of rotation, such as \mathbf{z} and \mathbf{v} . Thus U joints can be the virtual actuators with generalized coordinates α and β we are looking for. Of course, other solutions can exist, but U joints are the simplest ones.

If a U joint is the virtual actuator that makes the vector \mathbf{u}_i move, it is obvious that:

- if the value of \mathbf{u}_i is fixed, the U joint coordinates α and β must be constant, i.e. *the actuator must be blocked*,
- if the value of \mathbf{u}_i is changing, the U joint coordinates α and β must also vary.

As a result, to ensure the aforementioned properties for α and β if \mathbf{u}_i is expressed in the base or camera frame (but the problem is identical since the camera is considered fixed on the ground), vectors \mathbf{x} , \mathbf{y} and \mathbf{z} of Fig. 2(c) must be the vectors defining the base or camera frame. Thus, in terms of properties for the virtual actuator, this implies that the first U joint axis must be constant w.r.t. the base frame, i.e. the U joint must be attached to a link *performing a translation w.r.t. the base frame*².

However, in most of the cases, the real leg architecture is not composed of U joints attached on links performing a translation w.r.t. the base frame. Thus, the architecture of the hidden robot leg must be modified w.r.t. the real leg such as depicted in Fig. 2(b). The U joint must be mounted on a passive kinematic chain composed of at most 3 orthogonal passive P joints that ensures that the link on which is it attached performs a translation w.r.t. the base frame. This passive chain is also linked to the segments before the observed links so that they do not change their kinematic properties in terms of motion. Note that:

- it is necessary to fix the PPP chain on the preceeding leg links because the information given by the vectors \mathbf{u}_i is not enough for rebuilding the full platform position and orientation: it is also necessary to get information on the location of the anchor point A_{n-1} of the observed

²In the case where the camera is not mounted on the frame but on a moving link, the virtual U joint must be attached on a link performing a translation w.r.t. the considered moving link.

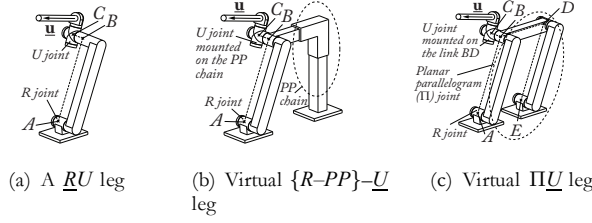


Fig. 3. An \underline{RU} leg and two equivalent solutions for its hidden leg

segment [17]. This information is kept through the use of the PPP chain fixed on the first segments;

- 3 P joints are only necessary if and only if the point A_{n-1} describes a motion in the 3D space; if not, the number of P joints can be decreased: for example, in the case of the GS platform presented in [13], the U joint of the leg to control was located on the base, i.e. there was no need to add passive P joints to keep the orientation of its first axis constant;
- when the vector \underline{u}_i is constrained to move in a plane such as for planar legs, the virtual actuator becomes an R joint which must be mounted on the passive PPP chain (for the same reasons as mentioned previously).

For example, let us have a look at the \underline{RU} leg with one actuated \underline{R} joint followed by a U joint of Fig. 3(a). Using the previous approach, its virtual equivalent leg should be an $\{R-PP\}-\underline{U}$ leg (Fig. 3(b)), i.e. the \underline{U} joint able to orientate the vector \underline{u}_i is mounted on the top of a $R-PP$ chain that can guarantee that:

- 1) the link on which the \underline{U} joint is attached performs a translation w.r.t. the base frame,
- 2) the point C (i.e. the centre of the U joint) evolves on a circle of radius l_{AB} , like the real leg.

It should be noticed that, in several cases for robots with a lower mobility (i.e. spatial robots with a number of dof less than 6, or planar robots with a number of dof less than 3), the last joint that links the leg to the platform should be changed so that, if the number of observed legs is inferior to the number of real legs, the hidden robot keeps the same number of controlled dof .

It should also be mentioned that we have presented above the most general methodology that is possible to propose, but it is not the most elegant way to proceed. In many cases, a hidden robot leg architecture can be obtained such that less modifications w.r.t the real leg are achieved. For example, the $R-PP$ chain of the hidden robot leg $\{R-PP\}-\underline{U}$ (Fig. 3(b)) could be equivalently replaced by a planar parallelogram (Π) joint without changing the aforementioned properties of the \underline{U} virtual actuator (Fig. 3(c)), i.e. only one additional joint is added for obtaining the hidden robot leg (note that we consider that a Π joint, even if composed of several pairs, can be seen as one single joint, as in [14]).

B. How to use the hidden robot models for analysing the controllability of the servoed robots

The aim of this Section is to show how to use the hidden robots for answering points 1 to 4 enumerated in the

introduction of the paper.

Point 1: the hidden robot model can be used to explain why the observed robot which is composed of n legs can be controlled using the observation of only m leg directions ($m < n$) arbitrarily chosen among its n legs, and can also help to choose the best set of legs to observe with respect to some given performance indices.

For answering this point, let us consider a general parallel robot composed of 6 legs (one actuator per leg) and having six dof . Using the approach proposed in Section III-A, each observed leg will lead to a modified virtual leg with at least one actuated \underline{U} joint that has two degrees of actuation. For controlling 6 dof , only 6 degrees of actuations are necessary, i.e. three actuated \underline{U} are enough. Thus, in a general case, only three legs have to be observed to fully control the platform dof .

Point 2: the hidden robot model can be used to prove that there does not always exist a full diffeomorphism between the Cartesian space and the leg direction space, but can also bring solutions for avoiding to converge to a non desired pose.

Here, the answer comes directly from the fact that the real controlled robot may have a hidden robot model with different geometric and kinematics properties. This means that the hidden robot may have assembly modes and singular configurations different from those of the real robot. If the initial and final robot configurations are not included in the same aspect (i.e. a workspace area that is singularity-free and bounded by singularities [2]), the robot won't be able to converge to the desired pose, but to a pose that corresponds to another assembly mode that has the same leg directions as the desired final pose.

Point 3: the hidden robot model simplifies the singularity analysis of the mapping between the leg direction space and the Cartesian space by reducing the problem to the singularity analysis of a new robot.

The interaction matrix \mathbf{M}^T involved in the controller gives the value of ${}^c\underline{u}$ as a function of ${}^c\tau_c$. Thus, \mathbf{M}^T is the inverse Jacobian matrix of the hidden robot (and, consequently, \mathbf{M}^{T+} is the hidden robot Jacobian matrix). Except in the case of decoupled robots [18], [19], [20], the Jacobian matrices of parallel robots are not free of singularities.

Thus,

- finding the condition for the rank-deficiency of \mathbf{M}^T is equivalent to finding the Type 2 (or parallel) singularities of the hidden robot [21],
- finding the condition for the rank-deficiency of \mathbf{M}^{T+} is equivalent to finding the Type 1 (or serial) singularities of the hidden robot [21].

Point 4: the hidden robot model can be used to certify that the robot will not converge to local minima.

The robot could converge to local minima if the matrix \mathbf{L}^{T+} of (6) is rank deficient. A necessary and sufficient condition for the rank deficiency of this matrix is that

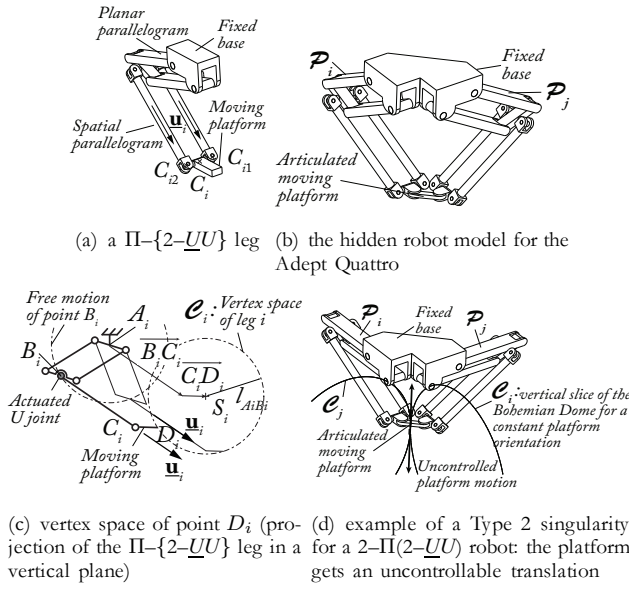


Fig. 4. Example of leg and of hidden robot for the Quattro

the \mathbf{M}^{T+} is rank deficient, i.e. the hidden robot model encounters a Type 1 singularity.

For illustrating this Section, let us present the *fkp* and singularity analysis of the hidden robot model of the Quattro with 4 *dof* (that can perform Schoenflies motions), when controlled using leg direction observation. It must be mentioned that, in [15], the Quattro with rigid platform, i.e. with 3 translation *dof*, was studied. The kinematics of the hidden robot for the version with 4 *dof* is completely different and is the object of this Section.

The Quattro is made of 4 $\underline{R}\text{--}\{2\text{--}\underline{US}\}$ legs (see Fig. 1), thus, following the previous approach, its equivalent hidden robot will be made of $\Pi\text{--}\{2\text{--}\underline{US}\}$ or $\Pi\text{--}\{2\text{--}\underline{UU}\}$ legs. As such hidden robot legs have 2 degrees of actuation (the \underline{U} joint is fully actuated), only two legs have to be observed for fully controlling the Quattro using leg direction observation. However in this case, if the hidden robot has a $2\text{--}\Pi\text{--}\{2\text{--}\underline{US}\}$ architecture, the platform will have two uncontrolled *dof*. This phenomenon disappears if $\Pi\text{--}\{2\text{--}\underline{UU}\}$ legs are used in the hidden robot model (Fig. 4 – in this picture, the articulated platform is simplified for a clearer drawing, but has indeed the kinematic architecture presented in Fig. 1(c)).

Forward kinematics and assembly modes. Without loss of generality, let us consider that we analyse the $2\text{--}\Pi\text{--}\{2\text{--}\underline{UU}\}$ robot depicted at Fig. 4(a). Looking at the vertex space of each leg when the active \underline{U} joints are fixed, the points C_i and D_i are carrying out a circle \mathcal{C}_i of radius $l_{A_iB_i}$ centred in S_i (Fig. 4(c)).

The Quattro with 4 *dof*, and consequently its hidden robot model, has a particularity: its platform is passively articulated (Fig. 1(c)) so that its orientation with respect to the horizontal plan xOy stays constant, while it can have one degree of rotation around the z axis, i.e. point D_2 can describe a circle \mathcal{C}_l located in the horizontal plane, centred in D_1 and with a

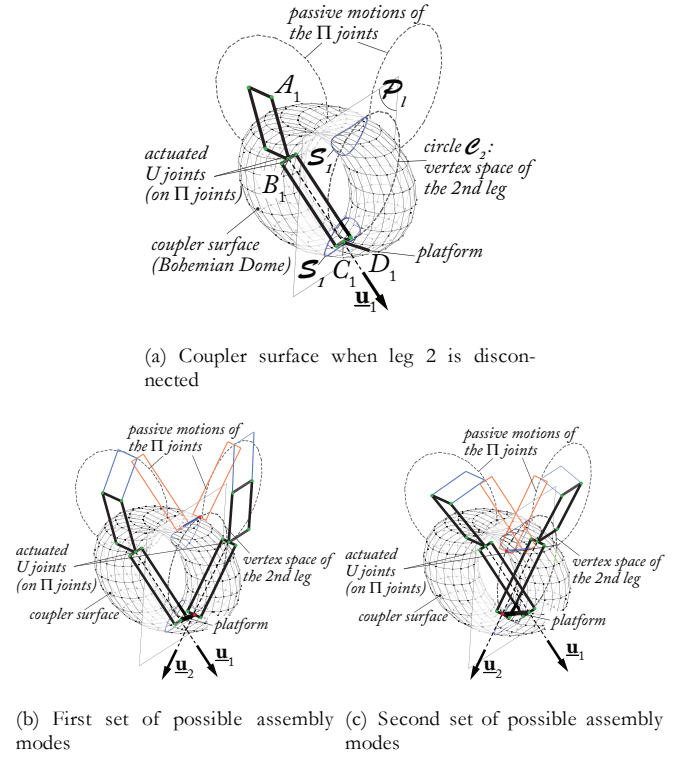


Fig. 5. Solutions of the *fkp* for a $2\text{--}\Pi\text{--}\{2\text{--}\underline{UU}\}$ robot (in this example, only 4 assembly modes exist)

radius $l_{D_1D_2}$. For solving the forward kinematics, it is thus necessary to virtually cut the platform at point D_2 and to compute the coupler surface of point D_2 when it belongs to leg 1. This coupler surface is the surface generated by \mathcal{C}_l when it performs a circular translation along \mathcal{C}_1 . Such a surface is depicted in Fig. 5(a) and is called a Bohemian Dome [22].

A Bohemian Dome is a quartic surface, i.e. an algebraic surface of degree 4. When it intersects the vertical plane \mathcal{P}_l containing the circle \mathcal{C}_2 (i.e. vertex space of the second leg), the obtained curve is a quartic curve (denoted at \mathcal{S}_1 – Fig. 5(a)). And using the Bézout theorem [23], it can be proven that, when the circle corresponding to the vertex space of leg 2 intersects this quartic curve, there can exist at most 8 intersection points, i.e. 8 assembly modes. Some examples of assembly modes for the $2\text{--}\Pi\text{--}\{2\text{--}\underline{UU}\}$ robot are depicted in Figs. 5(b) and 5(c).

Singular configurations. For the $2\text{--}\Pi\text{--}\{2\text{--}\underline{UU}\}$ robot, Type 2 singularities appear when the planes \mathcal{P}_i and \mathcal{P}_j (whose normal vectors are equal to $\underline{\mathbf{v}}_i^\perp$ and $\underline{\mathbf{v}}_j^\perp$, resp.) are parallel. In such cases, the circle \mathcal{C}_2 is tangent to the Bohemian Dome at their intersection point and the robot gains one uncontrollable *dof* along this tangent (Fig. 4(d)). We must note here that this can happen even when all four legs are being observed, so in some situations, stacking the interaction matrices is not a solution.

C. Selection of the Controlled Legs

This Section has shown the importance of studying the intrinsic properties of the controller that are directly related to the choice of the stacked interaction matrices required for computing the control law. Depending on the chosen interaction matrices, i.e. on the choice of the observed legs, the geometry of the hidden robot models will vary, as well as its singularities and assembly modes. As singularities divide the workspace into distinct aspects [2], it is necessary to study the motion feasibility by selecting a set of legs that can allow the robot displacement. Moreover, even if the motion is feasible, if the robot goes close to a singularity, the positioning error can considerably grow.

Therefore, it is necessary to find the best set of legs to observe in order to get the best performances of the robot w.r.t. a desired task. For the sake of compactness, the methodology for this will not be presented here, but the reader is referred to [15] for more information on this.

In the next Section, all the presented theoretical results are validated through experiments on the Adept Quattro [24].

IV. CASE STUDY

A. Description of the benchmark

In this Section, experiments are performed on the Adept Quattro presented in the previous Section. The benchmark is composed of (Fig. 6):

- an Adept Quattro robot bought by the Institut Pascal of Clermont-Ferrand (France),
- a camera AVT Marlin F131B firewire IEEE1394 (lens: 3.6mm 1:1.6 1/2 inch for CCD camera), which is mounted at the centre of the robot base so that all the legs can be observed without any problems of occlusion and whose intrinsic and extrinsic parameters have been calibrated,
- a lighting system that provides an homogeneous lighting to the scene,
- a computer that extracts the data coming from the camera, computes the value of the leg directions \underline{u} , then calculates the robot actuator velocity $\dot{\mathbf{q}}$ using the controller of Section II-B and send the information to the robot controller. Note that, in experiments, the value of λ in the controller is fixed to 0.2.

It must be mentioned we have deliberately decided to use the minimal camera resolution and not to correct the distortion of the captured image. The measurement noise on the leg direction is thus of about 0.1 rad, but:

- such a high noise is interesting to show the controller robustness to leg direction prediction errors,
- the noise is so high that, for analysing the robot accuracy and measuring the distance between the real and nominal robot configurations, we can directly record and use the value of the platform pose predicted by the Adept Quattro controller instead of using one external measurement device (such as a laser tracker).

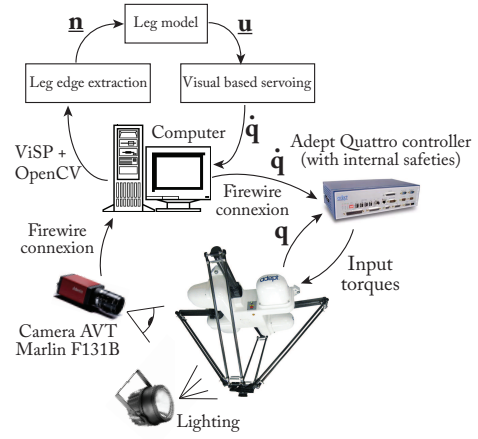


Fig. 6. Experimental bench

B. Experimental validations

Testing the convergence of the robot to the desired pose

In the first set of experiments, the initial platform pose is equal to $\{x = 0m, y = 0m, z = -0.75m, \phi = 0rad\}$ and the final desired platform pose is set to $\{x = -0.2m, y = 0m, z = -0.56m, \phi = 0rad\}$. To go from the initial point to the final one, two sets of observed leg directions are tested: $\{1, 4\}$ and $\{2, 3\}$. For those two sets of legs, solving the *fkp* of the hidden robot model of the Quattro presented in Section III-B at the desired final configuration of the robot, gives four possible solutions each. For legs $\{1, 4\}$, these are:

- $\{x = -0.2m, y = 0m, z = -0.56m, \phi = 0rad\}$
- $\{x = -0.2m, y = 0m, z = -0.909m, \phi = 0rad\}$
- $\{x = -0.138m, y = 0.062m, z = -1.019m, \phi = 0rad\}$
- $\{x = -0.138m, y = 0.062m, z = -0.45m, \phi = 0rad\}$

The solutions for legs $\{2, 3\}$ are:

- $\{x = -0.2m, y = 0m, z = -0.56m, \phi = 0rad\}$
- $\{x = -0.2m, y = 0m, z = -0.296m, \phi = 0rad\}$
- $\{x = -0.262m, y = 0.062m, z = -0.694m, \phi = 0rad\}$
- $\{x = -0.262m, y = 0.062m, z = -0.161m, \phi = 0rad\}$

The robot is asked to move from the initial configuration to the final one. Due to the presence of high measurement noise, the robot can of course not converge to the final desired pose.

The results are illustrated in Figs. 7 and 8. It can be seen that using legs $\{1, 4\}$, not all legs tend to go to zero, and indeed the final attained pose will be $P_{f14} = \{x = -0.11, y = 0.01, z = -0.86, \phi = -2.15rad\}$. Simulations were run by adding the measurement noise to the leg directions in the kinematic model [15] to determine the uncertainty areas due to the aforementioned measurement error corresponding to the final attained position. The resulting tolerable errors in position and orientation were 0.11m and 2.00rad, respectively. The *fkp* solution around P_{f14} is $\{x = -0.2m, y = 0m, z = -0.909m, \phi = 0rad\}$, so the

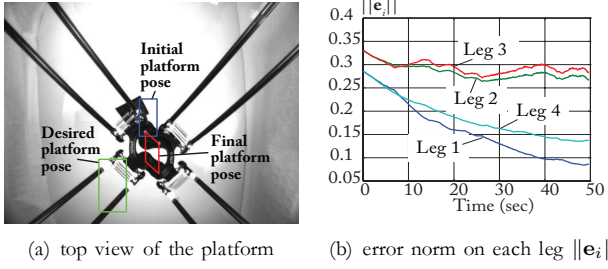


Fig. 7. Convergence of the robot when legs 1 and 4 are observed (desired pose: $\{x = -0.2, y = 0, z = -0.56, \phi = 0\}$).

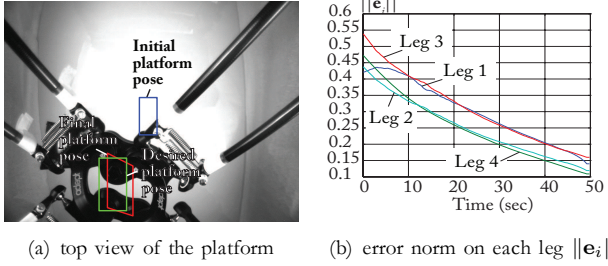


Fig. 8. Convergence of the robot when legs 2 and 3 are observed (desired pose: $\{x = -0.2, y = 0, z = -0.56, \phi = 0\}$).

robot does not converge to the desired pose, but to the second *fkp* solution of its hidden robot model.

When observing legs $\{2, 3\}$, all legs correctly tend to go to zero, and the final attained pose will be $P_{f23} = \{x = -0.12, y = 0.05, z = -0.55, \phi = -0.90rad\}$. After the simulations, we obtain the associated uncertainty area of this final pose, characterised by tolerable errors of $0.23m$ in position and $1.23rad$ in orientation. Around P_{f23} can be found the desired final position, i.e. the first *fkp* solution, $\{x = -0.2m, y = 0m, z = -0.56m, \phi = 0rad\}$.

A second experiment is performed in which all legs are observed. The initial platform pose is equal to $\{x = 0.05m, y = 0.05m, z = -0.8m, \phi = 0rad\}$ and the final desired platform pose is set to $\{x = 0.03m, y = 0.03m, z = -0.59m, \phi = 0rad\}$. Solving the *fkp* of the hidden robot model of the Quattro when all legs are observed at the desired final configuration of the robot, it can be proven that there still exist two assembly modes which are:

- $\{x = 0.03m, y = 0.03m, z = -0.59m, \phi = 0rad\}$
- $\{x = 0.03m, y = 0.03m, z = -0.65m, \phi = 0rad\}$

Performing the motion, the robot arrived in the final pose $P_{f1234} = \{x = 0.03m, y = 0.03m, z = -0.72m, \phi = 0.05rad\}$. Even though all legs tend to go to zero, the robot does not converge to the desired pose, but to the second *fkp* solution. Indeed, when we perform the simulations to determine the uncertainty area, we obtain tolerable errors in position of $0.08m$ and orientation of $1.54rad$, describing a volume which contains the aforementioned *fkp* solution, $\{x = 0.03m, y = 0.03m, z = -0.65m, \phi = 0rad\}$. The final platform pose presents an error of $0.07m$ in position error and $0.05rad$ in orientation w.r.t. this second *fkp* solution. These results are illustrated in Fig. 9.

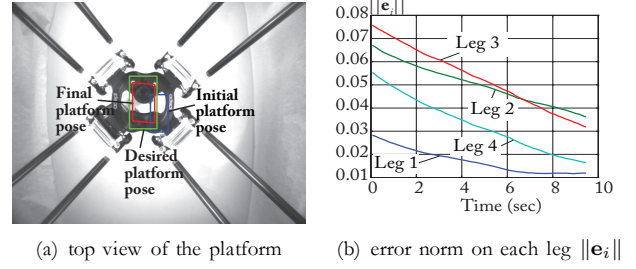


Fig. 9. Convergence of the robot when all legs are observed (desired pose: $\{x = 0.03, y = 0.03, z = -0.59, \phi = 0\}$).

It should be mentioned that the plotted values of the error norms are computed using the values of the leg directions given by the Quattro controller.

All these experimental results confirm the presence of the virtual robot hidden within the controller that must be studied in order to avoid the convergence problems due to inadequate stacking of interaction matrices.

Testing the importance of the selection of the observed legs on the robot accuracy

To show the importance of the leg selection on the robot accuracy, it is decided to control the robot displacement using different sets of legs. Each experiment is run five times and we present here the maximal values obtained on the position and orientation error.

In the first set of experiments, two different sets of legs are observed: (i) legs $\{2, 3\}$ and (ii) legs $\{2, 4\}$, going from the initial pose $\{x = 0.02m, y = 0.1m, z = -0.7m, \phi = 0rad\}$ to the final pose $\{x = -0.2m, y = 0.01m, z = -0.7m, \phi = 0rad\}$. When legs $\{2, 3\}$ are observed, the final pose accuracy shows a position error of $0.11m$ and an orientation error of $0.06rad$, while in the case of legs $\{2, 4\}$, the errors are $0.23m$ and $0.68rad$, respectively. Thus we obtain better accuracy when observing the first set of legs.

In the second set of experiments, the initial platform pose is equal to $\{x = 0.05m, y = 0.05m, z = -0.8m, \phi = 0rad\}$ and the final desired platform pose is set to $\{x = 0.03m, y = 0.03m, z = -0.65m, \phi = 0rad\}$. It is decided to control the robot displacement using three different sets of legs: (i) legs $\{1, 4\}$, (ii) legs $\{1, 3, 4\}$ and (iii) all legs. In the first case, the final platform pose is characterised by a $0.11m$ position error and a $0.39rad$ orientation error. When observing three legs, we obtain $0.09m$ error in position and 0.31 error in orientation. And lastly with four legs we have a position error of $0.07m$ and an orientation error of $0.05rad$. These results show that increasing the number of legs to be observed also increases the accuracy of the platform.

All these experimental results confirm the necessity to carefully select the set of legs to observe in order to obtain the best accuracy possible. However, it must be recalled that, even if observing all the legs lead to a better accuracy, this result must not hide the fact that some convergence problems can still appear, as shown previously.

V. CONCLUSIONS

This paper has presented the “hidden robot concept”, a tangible visualisation of the mapping between the observation space and Cartesian space of parallel robots controlled through the use of leg direction-based visual servoing. This robot, which has different assembly modes and singular configurations from the real robot, can be used as a tool to simplify the analysis of the mapping between intrinsic and extrinsic parameters acquired through vision. This tool offers:

- 1) explanation why it is possible to fully control the real robot by observing a number of legs which is less than the number of total legs,
- 2) proof that there does not always exist a full diffeomorphism between the Cartesian space and the leg direction space,
- 3) simplified singularity analysis of the mapping between the leg direction space and the Cartesian space by reducing the problem to the singularity analysis of a the new hidden robot,
- 4) knowledge about the existence of local minima and certification whether the robot will or will not converge to these, through the application of tools developed for the singularity analysis of robots.

A general approach has been presented, which allows the definition of the hidden robot model corresponding to any real parallel robot controlled via leg orientation-based visual servoing. This method has been applied to the Adept Quattro, followed by experiments which demonstrate the validity of the theoretical developments.

Finally, in this paper, we only considered to observe the leg direction \underline{u}_i , and not the leg edges in the image space, as the leg edges are only used as a measure of \underline{u}_i . However, *the problem is the same*, except in the fact that we must consider the singularity of the mapping between the edges and \underline{u}_i , which appears when the cylinders are at infinity [17].

Thus, the concept of hidden robot model has been proven to be a powerful tool, which brings mathematical tools developed by the mechanical design community to aid in the study of the correlation between intrinsic and extrinsic properties of some controllers developed by the visual servoing community. Also, not only has this tool simplified the analysis of the mapping between the Cartesian space and observation space, but has also proven that using only the extrinsic properties of the controller without doing the analysis of the intrinsic ones is clearly not enough.

REFERENCES

- [1] T. Leinonen, “Terminology for the theory of machines and mechanisms,” *Mechanism and Machine Theory*, vol. 26, 1991.
- [2] J. Merlet, *Parallel Robots*, 2nd ed. Springer, 2006.
- [3] —, 2012. [Online]. Available: www.sop.inria.fr/members/Jean-Pierre.Merlet/merlet.html
- [4] B. Espiau, F. Chaumette, and P. Rives, “A new approach to visual servoing in robotics,” *IEEE Transactions on Robotics and Automation*, vol. 8, no. 3, 1992.
- [5] R. Horaud, F. Dornaika, and B. Espiau, “Visually guided object grasping,” *IEEE Transactions on Robotics and Automation*, vol. 14, no. 4, pp. 525–532, 1998.
- [6] P. Martinet, J. Gallice, and D. Khadraoui, “Vision based control law using 3D visual features,” in *Proceedings of the World Automation Congress, WAC'96, Robotics and Manufacturing Systems*, vol. 3, Montpellier, France, May 1996, pp. 497–502.
- [7] E. Ozgur, N. Andreff, R. Dahmouche, and P. Martinet, “High speed parallel kinematic manipulator state estimation from legs observation,” in *Proceedings of the IEEE/RSJ International Conference on Intelligent Robots and Systems (IROS 2013)*, Tokyo Big Sight, Japan, 2013.
- [8] N. Andreff, A. Marchadier, and P. Martinet, “Vision-based control of a Gough-Stewart parallel mechanism using legs observation,” in *Proceedings of the IEEE International Conference on Robotics and Automation, ICRA'05*, Barcelona, Spain, April 18–22 2005, pp. 2546–2551.
- [9] V. Gough and S. Whitehall, “Universal tyre test machine,” in *Proceedings of the FISITA 9th International Technical Congress*, May 1962, pp. 117–317.
- [10] E. Ozgur, N. Andreff, and P. Martinet, “Dynamic control of the quattro robot by the leg edgels,” in *Proceedings of the IEEE International Conference on Robotics and Automation, ICRA11*, Shanghai, China, May 9–13 2011.
- [11] N. Andreff and P. Martinet, “Vision-based kinematic modelling of some parallel manipulators for control purposes,” in *Proceedings of EuCoMeS, the First European Conference on Mechanism Science*, Obergurgl, Austria, 2006.
- [12] F. Chaumette, *The Confluence of Vision and Control*, ser. LNCIS. Springer-Verlag, 1998, no. 237, ch. Potential problems of stability and convergence in image-based and position-based visual servoing, pp. 66–78.
- [13] S. Briot and P. Martinet, “Minimal representation for the control of Gough-Stewart platforms via leg observation considering a hidden robot model,” in *Proceedings of the 2013 IEEE International Conference on Robotics and Automation (ICRA 2013)*, Karlsruhe, Germany, May, 6–10 2013.
- [14] S. Caro, W. Khan, D. Pasini, and J. Angeles, “The rule-based conceptual design of the architecture of serial schonflies-motion generators,” *Mechanism and Machine Theory*, vol. 45, no. 2, pp. 251–260, 2010.
- [15] V. Rosenzweig, S. Briot, and P. Martinet, “Minimal representation for the control of the Adept Quattro with rigid platform via leg observation considering a hidden robot model,” in *Proceedings of the IEEE/RSJ International Conference on Intelligent Robots and Systems (IROS 2013)*, Tokyo Big Sight, Japan, 2013.
- [16] F. Chaumette, *La commande des robots manipulateurs*. Hermès, 2002.
- [17] N. Andreff, T. Dallej, and P. Martinet, “Image-based visual servoing of gough-stewart parallel manipulators using legs observation,” *International Journal of Robotics Research*, vol. 26, no. 7, pp. 677–687, 2007.
- [18] M. Carricato and V. Parenti-Castelli, “Singularity-free fully-isotropic translational parallel manipulators,” *International Journal of Robotics Research*, vol. 21, no. 2, pp. 161–174, 2002.
- [19] X. Kong and C. Gosselin, “A class of 3-dof translational parallel manipulators with linear input-output equations,” in *Proceedings of the Workshop on Fundamental Issues and Future Research Directions for Parallel Mechanisms and Manipulators*, Québec City, QC, Canada, October 2002, pp. 3–4.
- [20] G. Gogu, “Structural synthesis of fully-isotropic translational parallel robots via theory of linear transformations,” *European Journal of Mechanics. A/Solids*, vol. 23, no. 6, pp. 1021–1039, 2004.
- [21] C. Gosselin and J. Angeles, “Singularity analysis of closed-loop kinematic chains,” *IEEE Transactions on Robotics and Automation*, vol. 6, no. 3, pp. 281–290, 1990.
- [22] M. Tale Masouleh, C. Gosselin, M. Husty, and D. Walter, “Forward kinematic problem of 5-RPUR parallel mechanisms (3T2R) with identical limb structures,” *Mechanism and Machine Theory*, vol. 46, pp. 945–959, 2011.
- [23] E. Bézout, *Recherches sur le degré des équations résultantes de l'évanouissement des inconnues*. Histoire de l'Académie Royale des Sciences, 1764.
- [24] V. Nabat, M. de la O Rodriguez, O. Company, S. Krut, and F. Pierrot, “Par4: very high speed parallel robot for pick-and-place,” in *Proceedings of the 2005 IEEE/RSJ International Conference on Intelligent Robots and Systems (IROS 2005)*, 2005.